doi:10.1017/S1431927621002920
Microsc. Microanal. 27 (Suppl 1), 2021

Maximum thicknesses of EELS log ratio thickness measurement for several elements

Misa Hayashida[1] and Marek Malac[2]

[1]National Research of Council, Edmonton, Alberta, Canada, [2]National Research of Council, Alberta, Canada

Sample thickness (t) projected along the electron beam path can be measured in a transmission electron microscope (TEM) equipped with an energy filter for example by the log-ratio method. The relation underlying the log-ratio method is

$$t = \lambda \ln\left(\frac{I}{I_0}\right) \quad (1)$$

here t, λ, I and I_0 are sample thickness, inelastic mean free path (IMFP), total intensity of the incident beam and zero-loss filtered intensity [1, 2]. Eq. (1) can be applied to a pair of unfiltered and filtered images pixel by pixel providing a two-dimensional sample thickness map. We investigate the upper limit of the method when applied to thick samples. In particular, we are concerned with the maximum thickness yielding a linear dependence of $\ln(I/I_0)$ on t.

Aluminum and Epon exhibit linear response up to $\ln(I/I_0) < 5$ at 200 kV [3]. Al and Si linear dependence for $\ln(I/I_0) < \sim 1.2$, and Fe up to $\ln(I/I_0) < \sim 2.2$ at 200 kV with collection semi-angle (β) 11.9 − 35.7 mrad was reported in [4]. Ni, Al_2O_3, Si and SiO_2 linear dependence were limited to $\ln(I/I_0) < 0.5 - 0.6$ at 300 kV with β=17.7-25.1 mrad [5].

Alternatively, t can be measured by convergent beam electron diffraction (CBED)[1, 6, 7], Kramers-Kronig sum method [8, 9], and SEM [10, 11] Diameter of rod-shaped samples fabricated by a focus ion beam (FIB) was also used to estimate t at the center of rod-shaped samples[4, 5].

The maximum thickness t_{max} yielding linear response depends on collection semi-angle β and on the sample atomic number Z. We measured the relationships of $\ln(I/I_0)$-t for SiO_2, Al, Si, Ti, Ni, Cu, Ag and Au rectangular profile rod sample, see Fig. 1a, using a 300 kV Hitachi H9500 TEM with Gatan Tridiem™ electron energy filter. Slice sections from reconstructed images by electron tomography were used to measure local projected t precisely, see Fig. 1b. The dependence of $\ln(I/I_0)$ on t with β=16 mrad are shown in Fig 2a.

Fig. 2b shows plots of t_{max} extracted from Fig. 2a. The t_{max} decreases with increasing atomic number. The plots were fitted to $a+b*\log(Z)$. Here, Z is an atomic number, a and b are fit constants. Using this phenomenological fit, we it may be possible to predict t_{max} for other materials. The relationships the relationships of $\ln(I/I_0)$-t and t t_{max} were also measured for each material with β=3, 5, 9 and 99 mrad.

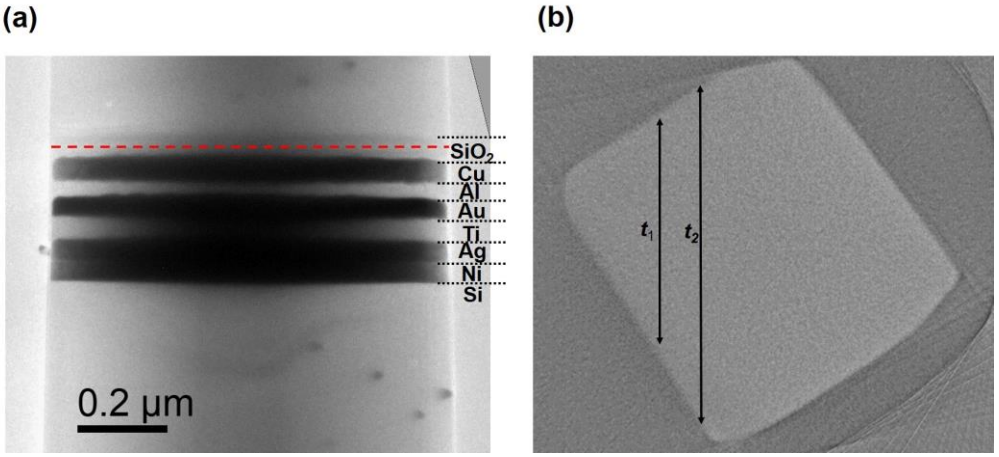

Figure 1. a) A TEM image of a rod-shaped multilayer sample fabricated by FIB. b) A slice section from a reconstructed 3D image of the sample in a). The slice section was extracted at location of the red dashed line in a). Two projected thicknesses t_1 and t_2 are indicated by arrows.

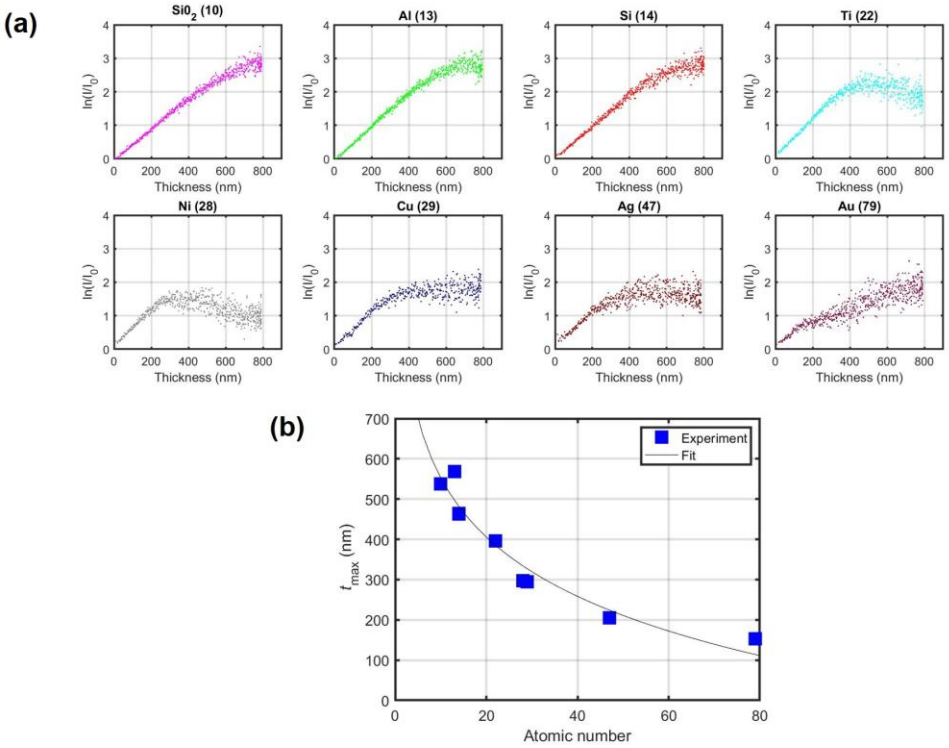

Figure 2. (a) Measured relationships of $\ln(I/I_0)$ vs.t for SiO_2, Al, Si, Ti, Ni, Cu, Ag with β=16 mrad, t was extracted at multiple locations as indicated in Fig 1b. (b) Maximum thickness t_{max} yielding a linear dependence of $\ln(I/I_0)$ on t from several element with β=16 mrad at 300 keV.

Reference

[1] T. Malis, S.C. Cheng, R.F. Egerton, EELS Log-ratio technique for specimen-thickness measurement in the TEM, Journal of Electron Microscopy Technique, 8 (1988) 193-200.

[2] R.F. Egerton, Electron Energy-Loss Spectroscopy in the Electron Microscope, 2 ed., Plenum Press, New York, 1996.

[3] J. Hosoi, T. Oikawa, M. Inoue, Y. Kokubo, K. Hama, Measurement of partial specific thickness (net thickness) of critical-point-dried cultured fibroblast by energy analysis, Ultramicroscopy, 7 (1981) 147-153.

[4] K. Oh-Ishi, T. Ohsuna, Inelastic mean free path measurement by STEM-EELS technique using needle-shaped specimen, Ultramicroscopy, 212 (2020) 112955.

[5] H. Meltzman, Y. Kauffmann, P. Thangadurai, M. Drozdov, M. Baram, D. Brandon, W.D. Kaplan, An experimental method for calibration of the plasmon mean free path, J. Microsc., 236 (2009) 165-173.

[6] P.L. Potapov, The experimental electron mean-free-path in Si under typical (S)TEM conditions, Ultramicroscopy, 147 (2014) 21-24.

[7] D.R.G. Mitchell, Determination of mean free path for energy loss and surface oxide film thickness using convergent beam electron diffraction and thickness mapping a case study using Si and P91 steel, Journal of Microscopy, 224 (2006) 187-196.

[8] K. Iakoubovskii, K. Mitsuishi, Y. Nakayama, K. Furuya, Thickness Measurements With Electron Energy Loss Spectroscopy, Microsc. Res. Tech., 71 (2008) 626-631.

https://doi.org/10.1017/S1431927621002920 Published online by Cambridge University Press

[9] K. Iakoubovskii, K. Mitsuishi, Mean free path of inelastic electron scattering in elemental solids and oxides using transmission electron microscopy: Atomic number dependent oscillatory behavior, PHYSICAL REVIEW B, 77 (2008) 104102.
[10] P. Zhang, Z. Wang, J.H. Perepezko, P.M. Voyles, Elastic and inelastic mean free paths of 200keV electrons in metallic glasses, Ultramicroscopy, 171 (2016) 89-95.
[11] D.T. Schweiss, J. Hwang, P.M. Voyles, Inelastic and elastic mean free paths from FIB samples of metallic glasses, Ultramicroscopy, 124 (2013) 6-12.

https://doi.org/10.1017/S1431927621002920 Published online by Cambridge University Press